11 Simulation of Gully Erosion and Bistable Landforms

ALAN D. HOWARD

Department of Environmental Sciences, University of Virginia, Charlottesville, Virginia, USA

11.1 INTRODUCTION

Accelerated erosion, including gully erosion, is a recurrent problem in most landscapes with deep regolith or soft bedrock. Rapid erosion is most commonly triggered by disruption of the vegetation cover by agricultural mismanagement, construction activities, fire, local landslides, or climatic change (see Schumm, this volume). In addition, erosion can be initiated by increased stress from overland flow due to changes in infiltration capacity or topographic changes concentrating flow, and less commonly, to extreme storm events. Once accelerated erosion has been initiated, return to a normal rate of erosion on all parts of the landscape may not occur until specific restorative actions are taken, such as seeding, fertilization, surface stabilization, grade control structures, and land recontouring. Incised valley bottoms are eventually stabilized due to lowered erosion rates and enhanced moisture availability (Ireland *et al.*, 1939). In some landscapes natural revegetation on gully walls and headcuts occurs when slope gradients drop below critical values for rapid failure, or when a year or two of frequent, low intensity rainstorms encourages vegetation establishment (Harvey, 1992; Alexander *et al.*, 1994). Most landscapes that are susceptible to accelerated erosion operate in a bistable erosional regime with the two metastable states of normal and accelerated erosion (Kirkby, 1995; Howard, 1997a). Bistable states are explored in this chapter within the context of a simple, spatially explicit simulation model.

Gully systems considered here develop in low-order channels, headwater hollows, and the lower portions of slopes (Figure 11.1). The development and erosion of gullies is generally distinguished from both smaller natural or human-induced rills on slopes and the cycles of entrenchment and filling in high-order channels and arroyos (Elliott *et al.*, this volume). Each of these landform suites has a voluminous and largely distinct literature despite their intergrading morphologies and similar erosional processes and controlling factors.

In most landscapes in humid climates the natural vegetation significantly restricts erosion by runoff due to root cohesion, an open soil structure that encourages infiltration, and a high surface roughness that diminishes runoff velocity (Thornes, 1985). The importance of this vegetative cover is made apparent when it is removed during construction, when erosion rates may increase by a factor of several hundred to ten thousand (Guy, 1965, 1972; Wolman, 1967; Vice *et al.*, 1968; Howard and Kerby, 1983). The deep regolith present throughout much of the south-eastern United States could only

Incised River Channels, Edited by S.E. Darby and A. Simon

have developed beneath a protective vegetation cover persisting during much of the Cenozoic (Pavich, 1989). Accelerated erosion in this region due to poor agricultural practices from colonial times through the beginning of this century transferred immense quantities of sediment from hillslopes to valley bottoms, often resulting in deep gullying and valley sedimentation of a metre or more (Ireland *et al.*, 1939; Happ *et al.*, 1940; Trimble, 1974; Jacobson and Coleman, 1986).

Figure 11.1 A gully system advancing through a broad hollow in the coast ranges of Northern California east of Point Reyes, USA. Some revegetation of the channel bottom is occurring even though the gully headwalls are still advancing.

Vegetation cover is often undervalued in terms of its control over landscape evolution. Its resistance to erosion, however, may be of the same order of magnitude as the underlying bedrock. In the Piedmont region of the south-eastern United States, bedrock is commonly exposed in low-order stream channels, whereas deep regolith occurs beneath slopes and divides. If these landscapes approximate steady state denudation, then erosion

of the hillslopes beneath a vegetative cover by creep and water erosion occurs only as rapidly as bedrock scour in nearby channels.

A vegetated landscape can thus be viewed as a three-layer structure: a thin vegetation cover, a more erodible regolith, and underlying bedrock. In some cases either the outer or inner layer may effectively be absent, as with unvegetated badlands in the case of the former, or deep unconsolidated sediments in the case of the latter. Where bedrock is exposed both outer layers are absent. Such a three-layer structure is incorporated in the present model. In some cases it may be necessary to incorporate a more complicated structure. For example, the B-horizon in soils in the south-eastern US often has greater erosional resistance than the overlying A-horizon, producing appreciable scarps in the clay-rich layer during gully incision (Ireland *et al.*, 1939). Hardpans, fragipan, calcrete, silcrete, and ferricrete layers may play similar roles in other soils (Poesen and Govers, 1990).

Reduction of erosional resistance through disturbance of the vegetation cover, either directly by fire, cultivation, overgrazing and so on, or indirectly by landslides, is a common cause of accelerated erosion (Thornes, 1985; Foster, 1990). In some cases, the enhanced erosion may instead arise from high stresses imposed by storm runoff, in part due to higher specific runoff yield and reduced hydraulic resistance where vegetation density is diminished (Graf, 1979; Bull, 1997). In order for erosion to continue to the point of producing a gullied landscape, re-establishment of vegetation must be inhibited; this inhibition is the second requirement for a bistable erosional regime. Several factors related to the rapid erosion following vegetation disturbance are responsible for this inhibition: physical undermining of vegetation by erosion, removal of the seed and nutrient reservoir of the upper soil layers, rapid drying of unvegetated soil, and high temperatures on sunlit soils, among others. The inhibition of vegetation recovery in areas of high erosion rates is incorporated in some ecological models (Williams *et al.*, 1984; Biot, 1990).

Accelerated erosion may also be triggered by rapid entrenchment of master drainage channels, creating migrating knickpoints on tributaries that encroach into headwater hollows and slopes. The entrenchment may be due either to human interference, such as channelization (Daniels, 1960; Daniels and Jordan, 1966) or overgrazing, or to climatic change (Brice, 1966). A general review of the controversy surrounding climatic versus anthropogenic control over gullying in the south-west US is provided by Cooke and Reeves (1976) and by Elliott *et al.* (this volume). Master-channel incision can be caused by vegetation degradation within the channel, for example, in the grass-covered cienega channels of the south-west US (Schumm and Hadley, 1957; Melton, 1965; Bull, 1997) and the Australian dambo channels (Boast, 1990; Prosser and Slade, 1994; Prosser *et al.*, 1994, 1995; Rutherfurd *et al.*, 1997). In this instance gully extension is just a larger example of the simulations presented here. Alternatively, incision may be due to unrelated causes such as climate change or base level change.

Evolution of bistable landscapes following disturbance is explored below using a 3-D simulation model, details of which are now provided.

11.2 THE DRAINAGE BASIN MODEL

The drainage basin model (Howard, 1994a) combines diffusive (mass wasting and rainsplash) plus advective (fluvial erosion) processes. Several 2-D (cross-sectional models) and 3-D (areally-explicit models) advection-dispersion landscape models have been developed (Kirkby, 1971; Hirano, 1975; Ahnert, 1976; Willgoose *et al.*, 1991), but the present model differs from most of these by assuming that headwater channels are detachment-limited (although Ahnert (1976) allows the possibility of similar 'suspended-load' runoff erosion). In detachment-limited erosion, sediment transport rates are less than flow capacity, and the erosion rate is limited by the ability of the flow to entrain surface materials, either due to soil cohesion or a vegetation cover. The difference between transport-limited and detachment-limited conditions has important implications for transient evolution of landscapes. Parallel slope retreat and development of basal pediments requires detachment-limited slopes and headwater channels, whereas transport-limited landscapes approach a 'characteristic form' in which gradients gradually wax or wane (Howard, 1994a; Willgoose, 1994). Formation of gullies of the type considered here requires detachment-limited erosion.

Potential erosion or deposition due to diffusive processes, $\left.\frac{\partial z}{\partial t}\right|_m$, is given by the spatial divergence of the vector flux of regolith movement, $\boldsymbol{q}_\mathbf{m}$

$$\left.\frac{\partial z}{\partial t}\right|_m = -\nabla \cdot \boldsymbol{q}_\mathbf{m} \tag{11.1}$$

The rate of movement is expressed by two additive terms, one for creep and/or rainsplash diffusion and one for rapid erosion as gradients approach a limiting value

$$\boldsymbol{q}_\mathbf{m} = \left[K_s \Gamma(S) + K_f \left(\frac{1}{1 - \left\{ |S| / S_t \right\}^a} - 1 \right) \right] \boldsymbol{s} \tag{11.2}$$

where $\Gamma(S)$ is an increasing function of slope gradient, $\boldsymbol{s}$ is the unit vector in the direction of $\boldsymbol{S}$, and $|S|$ is the absolute value of local slope gradient. The diffusivities K_s and K_f depend jointly upon regolith properties and climatic forcing and determine the overall rate of mass wasting. The model here assumes that $\Gamma(S)$ is simply the slope gradient, S. The term in parentheses in equation (11.2) models rapid mass movement such that long-term rates increase without limit as gradient approaches a limiting value S_t. The exponent a determines how rapidly mass movement rates increase as the limiting slope angle is approached. The constants K_s, S_t and K_f, and the exponent a are assumed to be spatially and temporally invariant.

The present model differs from the conceptual model of bistable badland landscapes envisioned by Kirkby (1995) in that erosion of devegetated slopes is assumed to be transport-limited with an active colluvial layer rather than being weathering-limited. For

the simulations considered here, the gullies are assumed to develop in a pre-existent deep regolith, or alternatively, to be incised into weak shale that is easily slaked to form a thin regolith, as in the badlands described by Howard (1994b, 1997b).

Fluvial erosion is advective, and consists of two processes: detachment-limited erosion for steep channels flowing on bedrock or regolith in which the bedload sediment flux is less than a capacity load; and transport-limited erosion in lower gradient alluvial channels. The erosion rate due to detachment, $\left.\frac{\partial z}{\partial t}\right|_c$, is assumed to be proportional to the shear stress, τ, exerted on the bed and banks by a dominant discharge

$$\left.\frac{\partial z}{\partial t}\right|_c = -K_t(\tau - \tau_c) \tag{11.3}$$

where τ_c is a critical shear stress and K_t is the bed erodibility. Many studies have suggested that gully incision occurs when erosional stress exceeds a critical threshold value and that the rate of gully advance correlates with the applied shear stress (Horton, 1945; Graf, 1979; Begin and Schumm, 1979; Foster, 1990; Rauws and Govers, 1988; Torri *et al.*, 1987; Vandaele *et al.*, 1996), or alternatively when a critical stream power is exceeded (Thorne and Zevenbergen, 1990). Critical values of shear stress have been utilized in DEM models of erosion susceptibility and channel head development (Dietrich *et al.*, 1992, 1993). Experimental studies of soil erosion are generally consistent with erosion rates being proportional to runoff shear stress (Ree and Palmer, 1949; Parthenaides, 1965; Jamison *et al.*, 1968; Arulanandan *et al.*, 1973; Akky and Shen, 1973) as is monitoring of erosion in badlands (Howard and Kerby, 1983).

Shear stress can be related to channel gradient and drainage area using equations of hydraulic geometry and steady, uniform flow as discussed by Howard (1994a)

$$\tau = \gamma R_h S \tag{11.4}$$

$$V = K_n R_h^{2/3} S^{1/2} / N \tag{11.5}$$

$$Q = K_p R_h W V \tag{11.6}$$

$$Q = K_a A^e \tag{11.7}$$

$$W = K_w Q^b \tag{11.8}$$

where γ is the unit weight of water, R_h is hydraulic radius, S is channel gradient, V is mean velocity, N is Manning's resistance coefficient, Q is an effective discharge, A is drainage area, and K_n, K_p, K_a and K_w are coefficients. These coefficients and exponents are assumed temporally and spatially invariant. These, when substituted into equation

(11.3) allow the erosion rate to be expressed as a function of drainage area and local gradient

$$\left.\frac{\partial z}{\partial t}\right|_c = -K_t\left(K_z A^f S^h - \tau_c\right), \text{ where} \tag{11.9a}$$

$$K_z = \gamma\left\{\frac{NK_a^{(1-b)}}{K_p K_w K_n}\right\}^{3/5} \tag{11.9b}$$

where K_z incorporates the various coefficients and constants in equations (11.4 to 11.8), and the exponents have the values $f = 0.6e(1\text{-}b)$ and $h = 0.7$. The values of K_z, K_t, f, and h are also assumed to be temporally and areally invariant. The rate of advance of gully and arroyo headcuts has been found to correlate with drainage area and/or channel gradient (Seginer, 1966; Patton and Schumm, 1975; Begin and Schumm, 1979; Schumm *et al.*, 1984; Moore *et al.*, 1988, Vandaele *et al.*, 1996). The detachment rate could alternatively be assumed to be proportional to other measures of flow strength, such as stream power, which has the effect of changing the exponents f and h to near unity in equation (11.4) and replacing τ_c with a critical stream power.

A variety of processes have been observed to operate at gully headwalls, including fluvial incision, seepage erosion (Howard and McLane, 1988), piping (Jones, 1971 and 1981; Bryan and Yair, 1982; Prosser and Abernethy, 1996), plunge-pool erosion (Stein and Julien, 1993; Moore *et al.*, 1994; Robinson and Hanson, 1994 and 1995; Bennett *et al.*, 1997; Hanson *et al.*, 1997, Stein *et al.*, 1997), and mass-wasting (Bradford *et al.*, 1973 and 1978; Blong *et al.*, 1982; Poesen and Govers, 1990). General reviews are provided by Gardner (1983), Poesen and Govers (1990), Bocco (1991), Dietrich and Dunne (1993), and Bull and Kirkby (1997). The relative importance of each process varies amongst different geologic, vegetation, and climatic environments, and each process depends somewhat differently upon flow and material properties. The assumption is made here that erosion rates due to the dominant processes correlate with shear stress (equation 11.3), or alternatively with drainage area and gradient (equation 11.9). Often seepage, piping, mass wasting and plunge-pool erosion at headwalls depend upon relief generated by channel incision occurring downstream from the headwall, and therefore indirectly upon the shear stress or stream power. Where seepage erosion dominates, however, drainage area may not be a good measure of subsurface discharge (Coelho Netto and Fernandes, 1990).

As opposed to detachment-limited erosion on slopes and in gully headwalls, the downstream portions of the channel network may have a loose sediment bed. In such transport-limited alluvial channels the potential rate of erosion (or deposition) equals the rate of downstream change of the volumetric unit bed sediment transport rate, q_{sb}

$$\left.\frac{\partial z}{\partial t}\right|_c = -\nabla q_{sb} \tag{11.10}$$

Many bedload and total load sediment transport equations can be expressed as a functional relationship between the two dimensionless parameters Φ and $1/\Psi$

$$\Phi = K_e \left\{ \frac{1}{\Psi} - \frac{1}{\Psi_c} \right\}^p \tag{11.11}$$

where

$$\Phi = \frac{q_{sb}}{\omega d(1-\mu)} \text{ and } \frac{1}{\Psi} = \frac{\tau}{(\gamma_s - \gamma)d} \tag{11.12}$$

In these equations q_{sb} is bed sediment transport rate in bulk volume of sediment per unit time per unit channel width, ω is the fall velocity of the sediment grains, d is the sediment grain size, μ is alluvium porosity, and γ is the unit weight of sediment grains. As discussed by Howard (1994a), equation (11.11) can be recast using equations (11.4 to 11.8) into a relationship between unit bed sediment discharge, q_{sb}, drainage area, and gradient

$$q_{sb} = K_q \left(\frac{K_z A^f S^h}{(\gamma_s - \gamma)d} - \frac{1}{\Psi} \right)^p \text{ and} \tag{11.13a}$$

$$K_q = \omega(1-\mu)dK_e \tag{11.13b}$$

where K_q is generally assumed constant, and K_z, f and h are the same coefficients as in equation (11.9). For transport in sand-bed channels with high suspended loads the exponent p has a value of about 3.0 and $1/\psi_c$ is a negligible correction (e.g. the Einstein-Brown formula; see Vanoni, 1975, p. 194). Elevation changes in alluvial channels are modelled as the divergence of sediment flux (equation 11.10), but sediment transport occurs only in the downstream direction, with channel width parameterized by equation (11.8), as discussed by Howard (1994a).

The model assumes that channels are either alluvial or bedrock, with transitions from bedrock to alluvial occurring when and where gradients decrease to values given by solving equation (11.13) for gradient. Erosion rates in bedrock channels are assumed to not depend upon sediment load, or alternatively, it is assumed that the sediment load correlates with drainage area. Some models of erosion in rills and gullies assume that the erosion rate in bedrock channels decreases gradually as sediment loads approach saturation (Foster and Meyer, 1975; Foster, 1990), whereas the present model and some others (Meyer and Wischmeier, 1969; Ahnert, 1976) assume abrupt transition from detachment-limited to transport-limited erosion rates. Arguments in support of the present approach are the observation in natural channels that spatial transitions from bedrock to alluvial cover (and the reverse) are abrupt and that erosion by sediment abrasion in

bedrock channels should depend positively upon the amount of sediment in transport (Wohl, this volume).

The simulations assume that the amount of erosion accomplished during an individual erosional event is small compared to the scale of the landform, so that the above processes can be approximated as being continuous. The actual erosion (or deposition) occurring at a point, $\partial z/\partial t$, is a weighted sum of the potential mass wasting and fluvial erosion rates, as discussed in Howard (1994a). Regolith delivered by mass wasting into channels is assumed to be more erodible than the bedrock by a factor X. Runoff yield is assumed areally uniform, but may vary between vegetated and bare areas. The critical shear stress, τ_c (equation 11.3), on regolith-covered areas is assumed to be governed by the state of the vegetation cover and may be temporally and spatially variable.

Table 11.1 Values of simulation parameters[a]

	Fig. 11.2	Fig. 11.4	Fig. 11.5	Fig. 11.6	Fig. 11.7	Fig. 11.8
K_{tu}	1.0	1.0	1.0	1.0	1.0	1.0
K_{td}		20.0	20.0	5.0	20.0	40.0
τ_{cu}	20.0	20.0	20.0	20.0	20.0	20.0
τ_{cd}		1.0	10.0	10.0	10.0	1.0
τ_{cx}		15.0	1.0	5.0		1.0
E_u		1.5	5.0	10.0	5.0	3.0
E_d		15.0	15.0	15.0	15.0	10.0

[a] Common simulation parameters are as follows: $E_n = 1.0$, $K_s = 1.0$, $K_f = 0.5$, $S_t = 25$, $a = 3$, $f = 0.3$, $h = 0.7$, $K_z = 1.0$, $p = 3.0$, $r = 0.5$, $s = 0.3$, $t = 0.7$, $\Psi_c = 0.0$, $K_v = 1.0$, $K_q = 0.1$, $X = 500$. Regolith is indefinitely thick for Figures 11.2, 11.4, 11.6 and 11.7, but is 25 units thick for Figure 11.8 (compared to a total relief of 550 units). Note that all figures referred to are located in the plate section.

An example of a steady state simulation generated by a constant rate of lowering of the lower boundary is shown in Figure 11.2 (see plate section). In this and the other simulations, the lower, level boundary is the base level control, the lateral boundaries are periodic (water and sediment crossing the boundary re-enter on the opposite side), and the upper boundary is no-flux, so that water and sediment cannot cross this boundary and it becomes a drainage divide. In addition, all channels are assumed initially non-alluvial with an erosion rate governed by equation (11.9). Initial conditions are a flat surface with a slight fractal perturbation. In this simulation, gradients are sufficiently low that the threshold mass wasting term in equation (11.2) is unimportant. A non-zero value of a critical shear stress, τ_c, is assumed, so that the divides are broadly rounded and eroded solely by creep (see Table 11.1 for values of simulation parameters). The critical shear stress is assumed to be determined by the state of the vegetation cover, which is assumed to have a constant value, τ_{cu}. In this simulation and the others presented below the values of the parameters are arbitrary; that is, they are not scaled to any particular landscape, but

are selected to give an initial drainage density on the simulated landscape such that both headwater channels and slopes are well represented.

11.2.1 Bistable Erosion

In the present simulation model, when the vegetation is undisturbed the critical shear stress, τ_c (equation 11.3), is assumed to be areally and temporally constant. However, the critical shear stress is assumed to also depend upon the rate of erosion in a threshold manner. This critical shear stress is assumed to have a high value, τ_{cu}, so long as the local erosion rate, E (or $-\partial z/\partial t$), is lower than a critical value, E_u. However, if erosion locally exceeds this rate, the critical shear stress drops to a lower value, τ_{cd}, until the erosion rate drops to a low value E_d, when it is assumed that the vegetation is able to become re-established and the critical shear stress is re-established at the undisturbed value, τ_{cu}. In addition, the intrinsic erodibility, K_t, may increase for bare (K_{td}) versus vegetated land surface (K_{tu}). When the erosion rate is governed by the disturbed critical shear stress, the specific runoff yield is assumed to be greater by a factor R than that of the undisturbed landscape, due to the reduction in infiltration capacity that accompanies vegetation disturbance. Indeed, enhanced runoff rates from sites of vegetation disturbance or removal have been noted in several studies (Graf, 1979; Prosser and Slade, 1994; Bull, 1997). Thus, two erosional states are possible at each location in the landscape, normal and accelerated (Figure 11.3). As is illustrated in Figure 11.3, there may be a range of steady-state erosion rates, E_n, with ($E_d < E_n < E_u$), such that the whole landscape might be in either the normal or the accelerated state depending upon the initial conditions.

Direct experimental measurements suggest values of critical shear stress of about 1000-2400 dynes cm^{-2} for undisturbed grasslands, dropping to about 700 dynes cm^{-2} for heavily disturbed vegetation (Reid, 1989; Prosser and Slade, 1994; Prosser and Dietrich, 1995; Prosser *et al.*, 1995). Bare soils have a critical shear stress of only about 200-400 dynes cm^{-2} (Prosser *et al.*, 1995; Reid, 1989), suggesting that the ratio of τ_{cu}/τ_{cd} ranges upwards from 3 to 10 or more.

The initial conditions for the simulations assume that erosion has been operating in the undisturbed state and that the landscape is in steady state adjustment to an erosion rate E_n ($E_n < E_d < E_u$) with a critical shear stress τ_{cu} (Figure 11.2, see plate section). A short-lived disturbance of the vegetation cover is assumed to occur due, perhaps, to fire, cultivation, or overgrazing. The duration of this disturbance, T_d, is assumed to be very short compared with the timescale for development of the steady state landscape, T_e. During the disturbance interval the critical shear stress is assumed to drop to a value, τ_{cx}, that is less than τ_{cu} but may be greater or less than τ_{cd}. Following this period of disturbance the vegetation is assumed to recover, so that the critical shear stress returns to its undisturbed value, τ_{cu}, except for those portions of the landscape where $E > E_u$. In the disturbed areas, fluvial erosion is governed by the value of the parameters τ_{cd} and K_{td}, until the erosion rate should drop to a value $E < E_d$, whereupon the undisturbed values of τ_{cu} and K_{tu} are re-established.

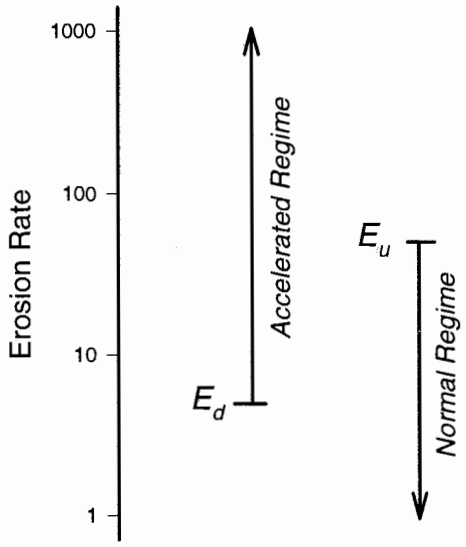

Figure 11.3 Conceptual diagram of the limits of stability of the normal and accelerated erosional regimes in bistable landscapes. Units for erosion rates are arbitrary and the transition erosion rates E_u and E_d are discussed in the text.

11.2.2 Example Simulations

Figure 11.2 (see plate section) shows the initial steady state landscape for all simulations developed in response to a constant rate of base level lowering. The time to steady state, T_e, is about 1500, about the time required to erode vertically an amount three times the steady state relief (Howard, 1994a; Ahnert, 1987; Fernandes and Dietrich, 1997). Although considerable erosion is required to attain steady state, the general arrangement and shape of channels and slopes is obtained when total erosion is only slightly more than the steady state relief. The patterns of gully erosion on non-steady state vegetated landscapes might be somewhat different than on steady-state landscapes. In most of the simulations, the easily eroded regolith or bedrock beneath the vegetation cover is assumed indefinitely thick.

Figure 11.4 (see plate section) shows a simulation in which the critical shear stress for the entire landscape is reduced for 0.01 time units by a factor of 0.75 ($\tau_{cx}/\tau_{cu} = 0.75$, see Table 11.1). The high erosion rates are triggered where and when erosion rates are 15

times higher than normal ($E_u/E_n = 15$). In these locations (brown areas) the ratio τ_{cu}/τ_{cd} is 20 and K_{td}/K_{tu} is 20. Runoff enhancement, R, on the disturbed portions of the landscape is five. Erosion only reverts to normal rates if the erosion rate drops below 1.5 times the normal value of unity ($E_d/E_n = 1.5$). Although the initial reduction in critical shear stress is moderate, the high assumed erodibility of bare regolith produces a steep wall of gullies and dissected slopes which propagates rapidly through the hollows and eventually onto the uplands. The steep gully sidewalls approach the critical angle S_t so that rapid mass wasting occurs. The rapid erosion rate and lower threshold cause an increase of drainage density in the disturbed portions of the landscape. The rapid erosion produces appreciable sedimentation in the valley bottoms (blue alluvial channels). In the later stages of the simulation, low erosion rates in the valley bottoms permit recolonization by vegetation (green areas). Parts of the recolonized valley bottom areas are former alluvial channel areas switching from deposition to erosion as sediment yields from the headwaters diminish.

In the simulation shown in Figure 11.4, the modest reduction in vegetational erosional resistance limited the initial dissection to channels and hollows. Figure 11.5 (see plate section) illustrates a scenario in which the reduction of critical shear stress is much greater ($\tau_{cx}/\tau_{cu} = 0.05$), so that most of the landscape goes into the high erosion rate state. Densely dissected, steep badlands similar in morphology to the Mancos Shale badlands of Utah (Howard, 1994b, 1997b) are eventually produced. If this simulation were continued beyond the stage shown in Figure 11.5b, a transient pediment would form in the valley bottoms (Howard, 1994a, 1997b). Because the simulation assumes that the base level continues to lower, however, the alluvial pediment would be short-lived, and vegetation would become re-established in the valley bottoms. Eventually there would be a slow return to a vegetated landscape similar to that in Figure 11.2 once the steep badland slopes had been stripped away.

Once the threshold to rapid erosion occurs within a landscape, reversion to the normal erosional state is difficult in the present model formulation. This is illustrated in Figure 11.6 (see plate section), in which the initial, short-duration reduction in critical shear stress is appreciable ($\tau_{cx}/\tau_{cu} = 0.25$), but the regolith is not as strongly erodible as in the previous cases ($\tau_{cu}/\tau_{cd} = 2$ and $K_{td}/K_{tu} = 5$). In addition, no enhancement of runoff from regolith slopes is assumed ($R = 1$), the erosion rate increase must be high to enter the rapid state ($E_u/E_n = 15$) and reversion to the normal state occurs at fairly high erosion rates ($E_d/E_n = 10$). Despite the modest enhancement factor for bare regolith erosion, the erosional 'shock front' passes through the entire landscape. After the shock front passes any given location, the slopes revert to normal erosion rates and a normal morphology.

Figure 11.7 (see plate section) shows the headward migration of an erosional shock front when the causative factor is a rapid lowering of base level (the lower boundary) rather than a lowering of critical shear stress. This case is distinguished from the previous ones primarily by the migration of the headcut through the channel system rather than the sudden incision of most of the channel network. In this simulation the rapid lowering is superimposed on the slow long-term incision. Again, if the simulation were continued a normal vegetated landscape would begin to form in the valley bottoms. If the incision were followed by base level stability, a pediment would form and extend headward (Howard, 1994a and 1997b).

When the regolith cover over bedrock is thin, the total incision is limited and gully extension proceeds slowly (Figure 11.8, see plate section).

11.3 DISCUSSION

A short-duration lowering of the critical shear stress for fluvial erosion may be sufficient to trigger accelerated erosion in landscapes with highly erodible regolith sandwiched between a resistant vegetation cover and bedrock. The accelerated erosion may continue over periods many times the duration of the initial disturbance. Incision rates are greatest on steep hillslopes and in hollows and low-order valleys, whereas divides and upper slopes may revert to normal erosion rates after the short duration of vegetational stress. Erosion in high-order valleys is limited by base level control. The locus of maximum erosion gradually works headward as a shock front and eventually may consume the divide areas, even though the disturbance initiating accelerated erosion might have lasted only a short while. If the vegetation undergoes no additional disturbance, erosion will eventually reduce gradients to the point that erosion rates will revert to the normal state. A different fate may occur if the regolith is thin, because bedrock will be exposed, and reversion to the previous state of thick regolith protected by vegetation would be difficult.

The proportion of the landscape which is triggered into accelerated erosion depends upon:

1. how much the erosion resistance offered by the vegetation cover is temporarily reduced (the ratio τ_{cx}/τ_{cu} in the simulations);
2. the relative shearing resistance and intrinsic erodibility of the regolith compared to the vegetated surface (τ_{cd}/τ_{cu} and K_{td}/K_{tu});
3. the rate of induced erosion which assures that the vegetation cannot become re-established by recovery of the normal vegetation (E_u);
4. the erosion rate at which vegetation recovery is assured following the cessation of disturbance (E_d); and
5. the degree to which specific runoff is enhanced in areas with disturbed vegetation (R).

The model also illustrates the two major approaches to controlling accelerated erosion: first through enhancement of the vegetation cover growth potential to reduce E_d, reduce runoff (R), and increase E_u; and second by protection of the surface to increase erosional resistance (increase τ_c) (Montgomery, this volume). Because steep, rapidly-eroding erosional fronts are created by the initial disturbance, uplands are progressively consumed by the advancing headwall even though the vegetation cover may be fully recovered. Thus structural treatments in the gullies (e.g. grade control structures and bank stabilization) are commonly required to halt their advance.

The model simulations clearly suggest that, once initiated, gullying in thick, erodible regolith or weak rocks may continue until all slopes are consumed by the wave of dissection if there is no intervention. In some environments, such unconstrained gullying and badland development may gradually consume the undisturbed areas. One well-known

example is the Badlands of South Dakota, which originated due to downcutting by the White River through Cenozoic shale and mudstone. These badlands have gradually advanced over thousands of years as a steep erosional front consuming a rolling, grassy upland (Figure 11.9). Dissection of the loess terrain of China has continued over a similar timespan (Zhu Xianmo, 1986). Gradual encroachment of gullies and badlands into vegetated slopes has continued over hundreds of years in Spain and Italy. In light of such examples, Bocco (1991) and Hudson (1985) suggest that gullying is not self-healing. On the other hand, inactive, naturally revegetated gullies can be found in many environments, such as the coastal ranges of California (Figure 11.10). Graf (1977) suggests that the rate of gully extension follows a negative exponential function, decreasing to zero as the gully approaches an equilibrium length, and Graf (1977), Prosser and Abernethy (1996), and Rutherford *et al.* (1997) present supporting data. This equilibrium length occurs when contributing area and slope drop below threshold values.

Figure 11.9 An advancing erosional front in the Badlands of South Dakota, USA. Remnants of the gently-rolling grassy upland surface are visible. The gullying was triggered by late Pleistocene downcutting of the master drainage, possibly aided by a drier Holocene climate that has reduced vegetation cover. As the upland is consumed by the narrow zone of advancing badland slopes, a pediment develops and extends headwards. The pediment in turn becomes vegetated and stabilized. In some locations additional master stream downcutting has caused dissection of the pediments as a second erosional front.

In the present model gullying continues until the entire landscape is consumed because fluvial incision in the unvegetated gullies maintains steep gradients. The main gullies extend through the channels and hollows and onto the lower sideslopes almost immediately after incision starts, however, with only minor extension as gullying gradually dissects the remaining hillslopes. Thus, the pattern of rapid followed by slow extension is not much different from that postulated by Graf (1977), except the steep shock front of incision eventually engulfs the entire landscape with a normal vegetated landscape reforming behind the shock front (Figure 11.6b, see plate section).

Gullying clearly ceases in many landscapes before the entire landscape is consumed. An example is shown in Figure 11.10. The steep, grassy landscape in the northern California Coast Ranges shown in Figure 11.10a has been dissected by two gullies occupying colluvial hollows. The gullying may have been initiated by vegetation disturbance or small landslides in the colluvial fill. The left gully in Figure 11.10a is undergoing active extension (Figure 11.10b), whereas the right gully (which is probably older) has become stabilized by vegetation (Figure 11.10c). The factors leading to the restabilization are uncertain, but may include diminished incision rates when incision of the main channel reached bedrock, the greater moisture supply in the gully floor encouraging vegetation regrowth, and wet seasons with abundant moisture but no strong storms.

(A)

Figure 11.10 Stable and active gullies in the coastal hills north of San Francisco, California, USA. (a) The left gully is actively extending headwards, whereas the right gully has become stabilized. Both gully systems occupy colluvial hollows.

(B)

(C)

Figure 11.10 (continued) (b) View looking downhill at the head of the left gully in (a). Note the abrupt headwall, the steep slopes undergoing rapid mass wasting, and the high drainage density on the headwall. Headwall retreat occurs both by runoff and shallow slumping as well as deeper rotational slumps. (c) View across the right gully in (a), showing the high vegetation density in the hollow, which has inhibited downcutting and promoted revegetation of the headwalls. Some localized headwall retreat is still occurring, as below and to the left of the figures. The causes for the contrast between the two gully systems are discussed in the text.

Several circumstances can curtail the universal landscape incision that occurs in the present simulations. Headward erosion of gullies in the landscape studied by Prosser and Abernethy (1966) ceases when the gullies incised into alluvium reach the base of the hillslopes, which are shallowly underlain by bedrock. The simulation shown in Figure 11.8 (see plate section) demonstrates how exposure of shallow bedrock slows gully extension. Exposure of bedrock limits the rate of incision below the gully headwall, often slowing its advance sufficiently to permit revegetation of the headwall. Exposure of bedrock may prevent plunge-pool erosion.

The model assumes spatially and temporally invariant erosion rate thresholds and spatially invariant critical shear stress. Spatial variation may occur in both erosion thresholds and critical shear stress. In semi-arid landscapes vegetation density and growth rates may be greatest in hollows and valley bottoms. As a result, the critical shear stress, τ_c, may be higher in valleys, as might be the erosion rate, E_u, required to initiate gully development. In some circumstances, gullies might develop on convex hillslopes while hollows and valleys remain stable despite their greater source drainage area. Gully incision also may increase the delivery of moisture to headwalls by groundwater seepage or baseflow, thus encouraging revegetation due to a higher erosion rate reversion to normal condition, E_d, not accounted for in the present model. This erosion rate transition, E_d, may also be time-dependent, increasing during wet periods. Revegetation can also be encouraged during periods of low erosion rates in intervals lacking major storm runoff. Finally, supply of subsurface water to headwalls extended by groundwater seepage may drop to zero as the channels become less incised upon reaching the upper portions of hollows and sideslopes. A possible approach to incorporating temporal variation in simulation parameters would be to utilize a stochastic precipitation forcing using an approach similar to that used by Benda and Dunne (1997) to model triggering of debris flows. High intensity rains would encourage incision by increasing the applied shear stress (high values of K_a in equation 11.7 and K_z in equation 11.9). Frequent low intensity events would encourage vegetation growth by increasing τ_c, E_u, and E_d, whereas droughts would have the opposite effect.

Some landscapes may experience natural epicycles of gully erosion without external forcing, possibly analogous to the cycles of colluvial infilling and landslide excavation in hollows in steep landscapes of the Pacific Rim (Dietrich and Dunne, 1978; Reneau and Dietrich, 1991; Benda and Dunne, 1997). In fact, the partial excavation of hollows by landslides can trigger further incision by gully extension. Such a mechanism might have triggered the gullies shown in Figures 11.1 and 11.10. Landsliding may not be a necessary trigger, however, because colluvial infilling of hollows may provide sufficient imbalance. Colluvial filling decreases the concavity of hollows, which increases gradients at the base of the hollow where contributing drainage area is the greatest, so that shear stresses are increased. In addition, the decreased concavity may reduce available moisture and thus the vegetation density.

The scale of focus in the present simulations has been on low-order channels, hollows, and hillslopes. A similar approach can be utilized to predict entrenchment in larger vegetated streams or unchanneled valleys, such as in cienegas (Leopold and Miller, 1956; Melton, 1965; Bull, 1997) and dambos (Boast, 1990; Prosser and Slade, 1994; Prosser *et al.*, 1994). In the present version of the model, sediment transport and deposition in

alluvial channels is assumed not to be influenced by vegetation. However, if channels have modest maximum flow intensities and a high frequency of low flows, vegetation (often grasses and sedges) may cover the channel bed. This reduces shear stresses on the bed and encourages sedimentation (Tsujimoto, this volume). However, as with the gullying discussed above, rapid incision into the vegetation cover can occur due to either high flow intensities or reduced vegetation density following droughts. This leads to a tendency for valley bottoms to alternate between periods of aggradation when flows are broad and shallow through abundant vegetation versus cycles of entrenchment in narrow, unvegetated incised channels. Such effects could be incorporated into the model through variable thresholds for sediment transport, $1/\Psi_c$. Bistable incision and aggradation influenced by vegetation may alternate not only temporally, but spatially as well in the guise of discontinuous gullies (Leopold and Miller, 1956; Schumm and Hadley, 1957; Blong, 1970; Bull, 1997).

The model is also limited in the degree to which it accurately models accelerated erosion. Incision of gullies often triggers secondary mechanisms of gully extension due to plunge-pool incision, slumping, piping, and seepage erosion not explicitly included in the model (but which could be incorporated if appropriate process laws are identified). Modelling of vegetation regrowth as being solely a function of incision rate is also suspect, as slope steepness, depth of incision (which might disfavour vegetation re-establishment by exposing infertile saprolite or through shadowing, or favour growth through greater moisture availability), aspect, and other factors might be important. Initiation of accelerated erosion can also be triggered by slope failures or large runoff events, which are not modelled in the examples presented.

The present model of bistable erosional processes is exploratory. The model might be made more realistic by addressing the above limitations as well as including stochastic runoff production and episodic variation in vegetation resistance to erosion and in recruitment probability. The effects of vegetation in low-order channels and hollows on thresholds for sediment transport, flow resistance, and rates of sediment deposition should be included in more realistic modelling. The vertical variability of regolith erosional susceptibility could also be incorporated to include, for example, resistant B-horizons, caliche, hardpans, etc.

Despite these limitations, spatially explicit models of gully development, such as that presented here, may prove to be practical tools for predicting landform degradation if properly calibrated. Such models might be used to identify locations most susceptible to gullying as well as to estimate the extent and rate of gully extension and amounts of sediment delivery.

In conclusion, the model illustrates the difficulty of control of accelerated erosion in bistable landscapes. Many natural landscapes illustrate the long duration of accelerated erosion and the shock-front progression of bare, rapidly eroding, gullied landscapes into metastable, gently rolling, and vegetated landscapes. In particular, the classic badlands of South Dakota are a narrow zone of steep dissection working headward into a grassy upland (Figure 11.9). Many other landscapes throughout the American West and elsewhere exhibit this dichotomy of adjacent, rapidly eroding badlands and smoother, stable, vegetated slopes in the same geologic unit.

11.4 REFERENCES

Ahnert, F. 1976. Brief description of a comprehensive three-dimensional process-response model of landform development. *Zeitschrift fur Geomorphologie, Supplementband*, **25**, 29-49.

Ahnert, F. 1987. Approaches to dynamic equilibrium in theoretical simulations of slope development. *Earth Surface Processes and Landforms*, **12**, 3-15.

Akky, M.R. and Shen, C.K. 1973. Erodibility of a cement-stabilized sandy soil. In: *Soil Erosion: Causes and Mechanisms*, Highway Research Board Special Report, **135**, 30-41.

Alexander, R., Harvey, A.M., Calvo, A., James, P.A. and Cerda, A. 1994. Natural stabilization mechanisms on badland slopes, Tibernas, Almeria, Spain. In: Millington, A.C. and Pye, K. (Eds), *Environmental Change in Drylands: Biogeographical and Geomorphological Perspectives*, John Wiley and Sons, Chichester, 85-111.

Arulanandan, K., Sargunam, A., Loganathan, P. and Krone, R.B. 1973. Application of chemical and electrical parameters to prediction of erodibility. In: *Soil Erosion: Causes and Mechanisms*, Highway Research Board Special Report, **135**, 42-51.

Begin, Z.B. and Schumm, S.A. 1979. Instability of alluvial valley floors: A method for its assessment. *Transactions of the American Society of Agricultural Engineers*, **22**, 347-350.

Benda, L. and Dunne, T. 1997. Stochastic forcing of sediment supply to channel networks from landsliding and debris flow. *Water Resources Research*, **33**, 2849-2863.

Bennett, S.J., Alonso, C.V., Prasad, S.N. and Romkens, M.J.M. 1997. Dynamics of head-cuts in upland concentrated flows. In: Wang, S.S.Y., Langendoen, E.J. and Shields, F.D. Jr. (Eds), *Management of Landscapes Disturbed by Channel Incision*, University of Mississippi, Oxford, Mississippi, 510-515.

Biot, Y. 1990. THEPROM – an erosion productivity model. In: Boardman, J., Foster, I.D.L. and Dearing, J.A. (Eds), *Soil Erosion on Agricultural Land*, John Wiley and Sons, Chichester, 465-479.

Blong, R.J. 1970. The development of discontinuous gullies in a pumice catchment. *American Journal of Science*, **268**, 369-384.

Blong, R.J., Graham, O.P. and Veness, J.A. 1982. The role of sidewall processes in gully development; some N.S.W. examples. *Earth Surface Processes and Landforms*, **7**, 381-385.

Boast, R. 1990. Dambos: A review. *Progress in Physical Geography*, **14**, 153-177.

Bocco, G. 1991. Gully erosion: processes and models. *Progress in Physical Geography*, **15**, 392-406.

Bradford, J.M., Farrell, D.A. and Larson, W.W. 1973. Mathematical evaluation of factors affecting gully stability. *Soil Science Society of America Proceedings*, **37**, 103-107.

Bradford, J.M., Piest, R.F. and Spomer, R.G. 1978. Failure sequence of gully headwalls in western Iowa. *Soil Science Society of America Journal*, **42**, 323-238.

Brice, J.C. 1966. Erosion and deposition in the loess-mantled Great Plains, Medicine Creek drainage basin, Nebraska. *US Geological Survey Professional Paper*, **352H**, 255-335.

Bryan, R.B. and Yair, A. (Eds) 1982. *Badland Geomorphology and Piping*, Geobooks, Norwich.

Bull, W.B. 1997. Discontinuous ephemeral streams. *Geomorphology*, **19**, 227-276.

Bull, L.J. and Kirkby, M.J. 1997. Gully processes and modelling. *Progress in Physical Geography*, **21**, 354-374.

Coelho Netto, A.L. and Fernandes, N.F. 1990. Hillslope erosion, sedimentation, and relief inversion in SW Brazil: Bananal, SP. *International Association of Scientific Hydrology Publication*, **192**, 174-182.

Cooke, R.U. and Reeves, W.R. 1976. *Arroyos and Environmental Change in the American South-West*, Clarendon Press, Oxford.

Daniels, R.B. 1960. Entrenchment of the Willow Drainage Ditch, Harrison County, Iowa. *American Journal of Science*, **258**, 161-176.

Daniels, R.B. and Jordan, R.H. 1966. Physiographic history and the soils, entrenched stream systems and gullies, Harrison County, Iowa. *US Department of Agriculture, Technical Bulletin,* **1348.**

Dietrich, W.E. and Dunne, T. 1978. Sediment budget for a small catchment in mountainous terrain. *Zeitschrift fur Geomorphologie, Supplementband,* **29**, 191-206.

Dietrich, W.E. and Dunne, T. 1993. The channel head. In: Beven, K. and Kirkby, M.J. (Eds), *Channel Network Hydrology*, John Wiley and Sons, Chichester, 175-219.

Dietrich, W.E., Wilson, C.J., Montgomery, D.R., McKean, J. and Bauer, R. 1992. Erosion threshold and land surface morphology. *Geology*, **20**, 675-679.

Dietrich, W.E., Wilson, C.J., Montgomery, D.R. and McKean, J. 1993. Analysis of erosion thresholds, channel networks and landscape morphology using a digital terrain model. *Journal of Geology,* **101**, 259-278.

Fernandes, N.F. and Dietrich, W.E. 1997. Hillslope evolution by diffusive processes: the timescale for equilibrium adjustments. *Water Resources Research,* **33,** 1307-1318.

Foster, G.R. 1990. Process-based modelling of soil erosion by water on agricultural land. In: Boardman, J., Foster, I.D.L. and Dearing, J.A. (Eds), *Soil Erosion on Agricultural Land,* John Wiley and Sons, Chichester, 429-445.

Gardner, T.W. 1983. Experimental study of knickpoint migration and longitudinal profile evolution in cohesive, homogeneous material. *Geological Society of America Bulletin,* **94**, 664-672.

Graf, W.L. 1977. The rate law in fluvial geomorphology. *American Journal of Science,* **277**, 178-191.

Graf, W.L. 1979. The development of montane arroyos and gullies. *Earth Surface Processes,* **4**, 1-14.

Guy, H.P. 1965. Residential construction and sedimentation at Kensington, Maryland. In: *Federal Inter-Agency Sedimentation Conference Proceedings, 1963,* US Department of Agriculture Miscellaneous Publication, **970,** 30-37.

Guy, H.P. 1972. Urban sedimentation – in perspective. *Journal of the Hydraulics Division of the American Society of Civil Engineers,* **98**, 2009-2016.

Hanson, G.J., Robinson, K.M. and Cook, K.R. 1997. Experimental flume study of headcut migration. In: Wang, S.S.Y., Langendoen, E.J. and Shields, F.D. Jr. (Eds), *Management of Landscapes Disturbed by Channel Incision,* University of Mississippi, Oxford, Mississippi, 503-509.

Happ, S.C., Rittenhouse, G. and Dobson, G.C. 1940. Some principles of accelerated stream and valley sedimentation. *US Department of Agriculture, Technical Bulletin,* **695**.

Harvey, A.M. 1992. Process interactions, temporal scales and the development of hillslope gully systems: Howgill Fells, northwest England. *Geomorphology,* **5,** 323-344.

Hirano, M. 1975. Simulation of developmental process of interfluvial slopes with reference to graded form. *Journal of Geology*, **83**, 111-123.

Horton, R.E. 1945. Erosional development of streams and their drainage basins: hydrophysical approach to quantitative morphology. *Geological Society of America Bulletin,* **56**, 275-370.

Howard, A.D. 1994a. A detachment-limited model of drainage basin evolution. *Water Resources Research*, **30**, 2261-2285.

Howard, A.D. 1994b. Badlands. In: Abrahams, A. and Parsons, A. (Eds), *Geomorphology of Desert Environments*, Chapman and Hall, London, 213-242.

Howard, A.D. 1997a. Simulation of gully erosion and bistable landforms. In: Wang, S.S.Y., Langendoen, E.J. and Shields, F.D. Jr. (Eds), *Management of Landscapes Disturbed by Channel Incision,* University of Mississippi, Oxford, Mississippi, 516-521.

Howard, A.D. 1997b. Badland morphology and evolution: interpretation using a simulation model. *Earth Surface Processes and Landforms*, **22**, 211-227.

Howard, A.D. and Kerby, G. 1983. Channel changes in badlands. *Geological Society of America Bulletin*, **94**, 739-752.

Howard, A.D. and McLane, C.F. 1988. Erosion of cohesionless sediment by groundwater seepage. *Water Resources Research*, **24**, 1659-1674.

Hudson, N.W. 1985. *Soil Conservation*, Batsford, London.

Ireland, H.A., Sharpe, C.F.S. and Eargle, D.H. 1939. Principles of gully erosion in the Piedmont of South Carolina. *US Department of Agriculture, Technical Bulletin*, **633**.

Jacobson, R.B. and Coleman, D.J. 1986. Stratigraphy and recent evolution of Maryland Piedmont flood plains. *American Journal of Science*, **268**, 613-637.

Jamison, V.C., Smith, D.D. and Thornton, J.E. 1968. Soil and water research on a claypan soil. *US Department of Agriculture, Technical Bulletin*, **1379**.

Jones, J.A.A. 1971. Soil piping and stream channel initiation. *Water Resources Research*, **7**, 602-610.

Jones, J.A.A. 1981. *The Nature of Soil Piping – A Review of Research*, British Geomorphological Research Group Monograph, **3**, Geobooks, Norwich.

Kirkby, M. J. 1971. Hillslope process-response models based on the continuity equation. *Special Publication, Institute of British Geographers*, **3**, 15-30.

Kirkby, M.J. 1995. Modelling the links between vegetation and landforms. *Geomorphology*, **13**, 319-335.

Leopold, L.B. and Miller, J.P. 1956. Ephemeral streams. Hydraulic factors and their relation to the drainage net. *US Geological Survey Professional Paper*, **282-A**.

Melton, M.A. 1965. The geomorphic and paleoclimatic significance of alluvial deposits in southern Arizona. *Journal of Geology*, **73**, 1-38.

Meyer, L.D. and Wischmeier, W.H. 1969. Mathematical simulation of the process of soil erosion by water. *Transactions of the American Society of Agricultural Engineers*, **18**, 448-453.

Moore, I.D., Burch, G.J. and MacKenzie, D.H. 1988. Topographic effects on the distribution of surface soil water and the location of ephemeral gullies. *Transactions of the American Society of Agricultural Engineers*, **31**, 1098-1107.

Moore, J.S., Temple, D.M. and Kirsten, H.A.D. 1994. Headcut advance threshold in earth spillways. *Bulletin of the Association of Engineering Geologists*, **31**, 277-280.

Parthenaides, E. 1965. Erosion and deposition of cohesive soils. *Journal of the Hydraulics Division of the American Society of Civil Engineers*, **91**, 105-139.

Patton, P.C. and Schumm, S.A. 1975. Gully erosion, northwest Colorado: A threshold phenomenon. *Geology*, **3**, 88-90.

Pavich, M.J. 1989. Regolith residence time and the concept of surface age of the Piedmont "peneplain". *Geomorphology*, **2**, 181-196.

Poesen, J. and Govers, G. 1990. Gully erosion in the loam belt of Belgium: typology and control measures. In: Boardman, J., Foster, I.D.L. and Dearing, J.A. (Eds), *Soil Erosion on Agricultural Land*, John Wiley and Sons, Chichester, 513-530.

Prosser, I.P. and Abernethy, B. 1996. Predicting the topographic limits to a gully network using a digital terrain model and process thresholds. *Water Resources Research*, **32**, 2289-2298.

Prosser, I.P. and Dietrich, W.E. 1995. Field experiments on erosion by overland flow and their implication for a digital terrain model of channel initiation. *Water Resources Research*, **31**, 2867-2876.

Prosser, I.P. and Slade, C.J. 1994. Gully formation and the role of valley-floor vegetation, south-eastern Australia. *Geology*, **22**, 1127-1130.

Prosser, I.P., Chappell, J. and Gillespie, R. 1994. Holocene valley aggradation and gully erosion in headwater catchments, south-eastern highlands of Australia. *Earth Surface Processes and Landforms*, **19**, 465-480.

Prosser, I.P., Dietrich, W.E. and Stevenson, J. 1995. Flow resistance and sediment transport by concentrated overland flow in a grassland valley. *Geomorphology,* **13**, 71-86.

Rauws, G. and Govers, G. 1988. Hydraulic and soil mechanical aspects of rill generation on agricultural soils. *Journal of Soil Science,* **39**, 111-124.

Ree, W.O. and Palmer, V.J. 1949. Flow of water in channels protected by vegetative linings. *US Department of Agriculture, Technical Bulletin,* **967**.

Reid, L.M. 1989. Channel formation by surface runoff in grassland catchment. Unpublished Ph.D. thesis, University of Washington, Seattle.

Reneau, S.L. and Dietrich, W.E. 1991. Erosion rates in the southern Oregon Coast range: evidence for an equilibrium between hillslope erosion and sediment yield. *Earth Surface Processes and Landforms*, **16**, 307-322.

Robinson, K.M. and Hanson, G.J. 1994. A deterministic headcut advance model. *Transactions of the American Society of Agricultural Engineers,* **37**, 1437-1443.

Robinson, K.M. and Hanson, G.J. 1995. Large-scale headcut erosion testing. *Transactions of the American Society of Agricultural Engineers,* **38**, 429-434.

Rutherfurd, I.D., Prosser, I.P. and Davis, J. 1997. Simple approaches to predicting rates of gully development. In: Wang, S.S.Y., Langendoen, E.J. and Shields, F.D. Jr. (Eds), *Management of Landscapes Disturbed by Channel Incision,* University of Mississippi, Oxford, Mississippi, 1125-1130.

Schumm, S.A. and Hadley, R.F. 1957. Arroyos and the semiarid cycle of erosion. *American Journal of Science,* **255**, 164-174.

Schumm, S.A., Harvey, M.D. and Watson, C.C. 1984. *Incised Channels: Morphology, Dynamics and Control,* Water Resources Publications, Littleton, Colorado.

Seginer, I. 1966. Gully development and sediment yield. *Journal of Hydrology,* **4**, 236-253.

Stein, O.R. and Julien, P.Y. 1993. A criterion delineating the mode of headcut migration. *Journal of the Hydraulics Division of the American Society of Civil Engineers,* **119**, 37-50.

Stein, O.R., Julien, P.J. and Alonso, C.V. 1997. Headward advancement of incised channels. In: Wang, S.S.Y., Langendoen, E.J. and Shields, F.D. Jr. (Eds), *Management of Landscapes Disturbed by Channel Incision,* University of Mississippi, Oxford, Mississippi, 497-502.

Thorne, C.R. and Zevenbergen, L.W. 1990. Prediction of ephemeral gully erosion on cropland of the south-eastern United States. In: Boardman, J., Foster, I.D.L. and Dearing, J.A. (Eds), *Soil Erosion on Agricultural Land,* John Wiley and Sons, Chichester, 447-460.

Thornes, J.B. 1985. The ecology of erosion. *Geography,* **70**, 222-236.

Torri, D., Sfalanga, M. and Chisci, G. 1987. Threshold conditions for incipient rilling. *Catena Supplement,* **8**, 97-105.

Trimble, S.W. 1974. *Man-Induced Soil Erosion on the Southern Piedmont, 1700-1970*, Soil Conservation Society, Ankemy, Iowa.

Vandaele, K., Poesen, J., Govers, G. and van Wesemael, B. 1996. Geomorphic threshold conditions for ephemeral gully incision. *Geomorphology,* **16**, 161-173.

Vanoni, V.A. (Ed), 1975. *Sedimentation Engineering,* American Society of Civil Engineers, New York.

Willgoose, G., 1994. A physical explanation for an observed area-slope-elevation relationship for declining catchments. *Water Resources Research*, **30**, 151-159.

Willgoose, G., Bras, R.L. and Rodriguez-Iturbe, I. 1991. A coupled channel network growth and hillslope evolution model, 1, Theory. *Water Resources Research*, **27**, 1671-1684.

Williams, J.R., Jones, C.A. and Dyke, P.T. 1984. A modelling approach to determining the relationship between erosion and soil productivity. *Transactions of the American Society of Agricultural Engineers,* **27**, 129-144.

Wolman, M.G. 1967. A cycle of sedimentation and erosion in urban river channels. *Geografiska Annaler,* **49A**, 385-395.

Zhu Xianmo (Ed). 1986. *Land Resources on the Loess Plateau of China,* Northwest Institute of Soil and Water Conservation, Acad. Sinica, Shaanxi Science and Technique Press.

APPENDIX: NOTATION

A	Drainage area
a	Exponent in rapid mass wasting term
b	Exponent in relationship between channel width and contributing area
d	Sediment grain size
E_n	The normal rate of base level lowering and the steady state erosion rate
E_d	The erosion rate above which the critical shear stress changes to τ_{cd}
E_u	The erosion rate below which the critical shear stress changes to τ_{cd}
e	Exponent in relationship between discharge and contributing area
f	Exponent for area in fluvial erosion relationship
h	Exponents for gradient in fluvial erosion relationship
K_a	Specific yield of runoff
K_e	Sediment transport coefficient
K_f	Rapid mass wasting diffusivity
K_n	Manning's equation coefficient
K_p	Channel form factor
K_q	Coefficient in sediment transport equation
K_s	Creep diffusivity
K_t	Intrinsic fluvial erodibility of surface materials
K_{tu}	Intrinsic erodibility of normal vegetated surface
K_{td}	Intrinsic erodibility of surface with disturbed vegetation
K_w	Channel width coefficient
K_z	Shear stress coefficient
N	Manning's resistance coefficient
p	Exponent in sediment transport equation
Q_w	Water discharge
q_m	Volumetric flux rate of mass movement
q_{sb}	Volumetric sediment transport rate
R	Enhancement factor for runoff on disturbed land surface
R_h	Hydraulic radius of channel flow
S	Slope gradient
S_t	Critical slope gradient
V	Mean flow velocity
T	Simulation time (arbitrary units)
T_d	Duration of lowering of erosion threshold to value τ_{cx}
W	Channel width
X	Relative erodibility of regolith and bedrock
$-\partial z/\partial t$	Erosion rate
$\Gamma(S)$	A function of slope gradient
γ	Fluid unit weight
γ_s	Sediment unit weight

μ	Alluvium porosity
τ	Shear stress on land surface generated by runoff
τ_c	Critical shear stress for erosion by fluvial detachment
τ_{cu}	The normal, undisturbed critical shear stress for fluvial erosion
τ_{cd}	The critical shear stress when the vegetation cover is removed or disturbed
τ_{cx}	The critical shear stress during a short initial period of disturbance
Φ	Dimensionless sediment transport rate
$1/\Psi$	Dimensionless shear stress
$1/\Psi_c$	Dimensionless critical shear stress for sediment transport
ω	Sediment particle fall velocity in fluid

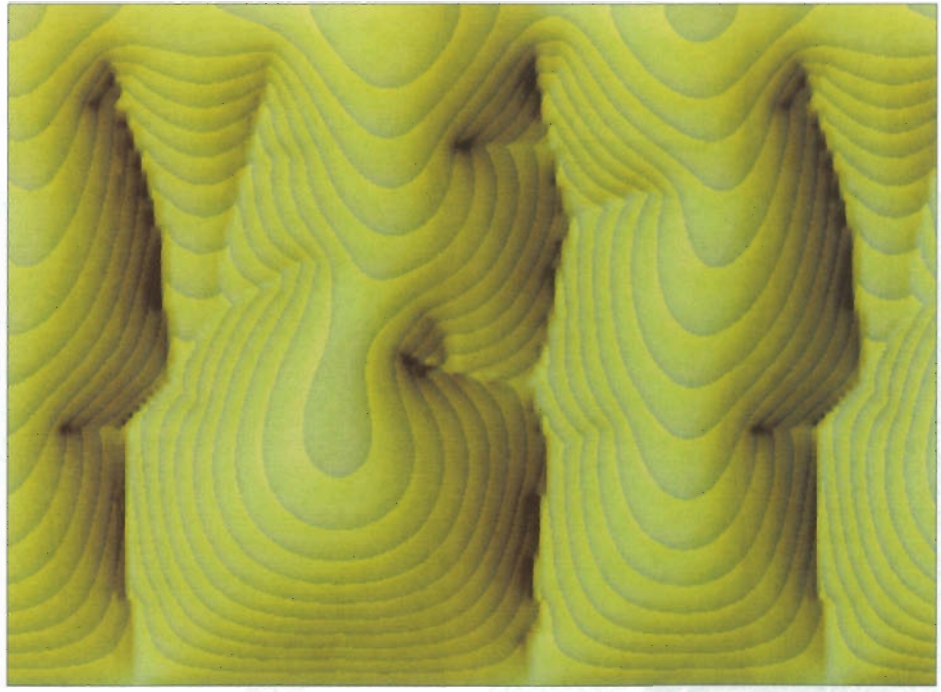

Figure 11.2 Simulation of a steady state landscape. No transport of water or mass occurs across the top boundary. The lateral boundaries are periodic, such that water and sediment exiting one side enters the opposite side, but portions of the matrix edges have been pasted to the opposite edges to make the morphology clearer. The lower boundary is lowered at a constant rate ($E_n = 1.0 = -\frac{\partial z}{\partial t}$). The assumption of a critical shear stress for fluvial erosion limits the extent of the drainage network and creates convex slope profiles. The total relief of the landscape is 520 (arbitrary units) and the contour interval is 32 in this and subsequent illustrations. Values of simulation parameters for all figures are shown in Table 11.1.

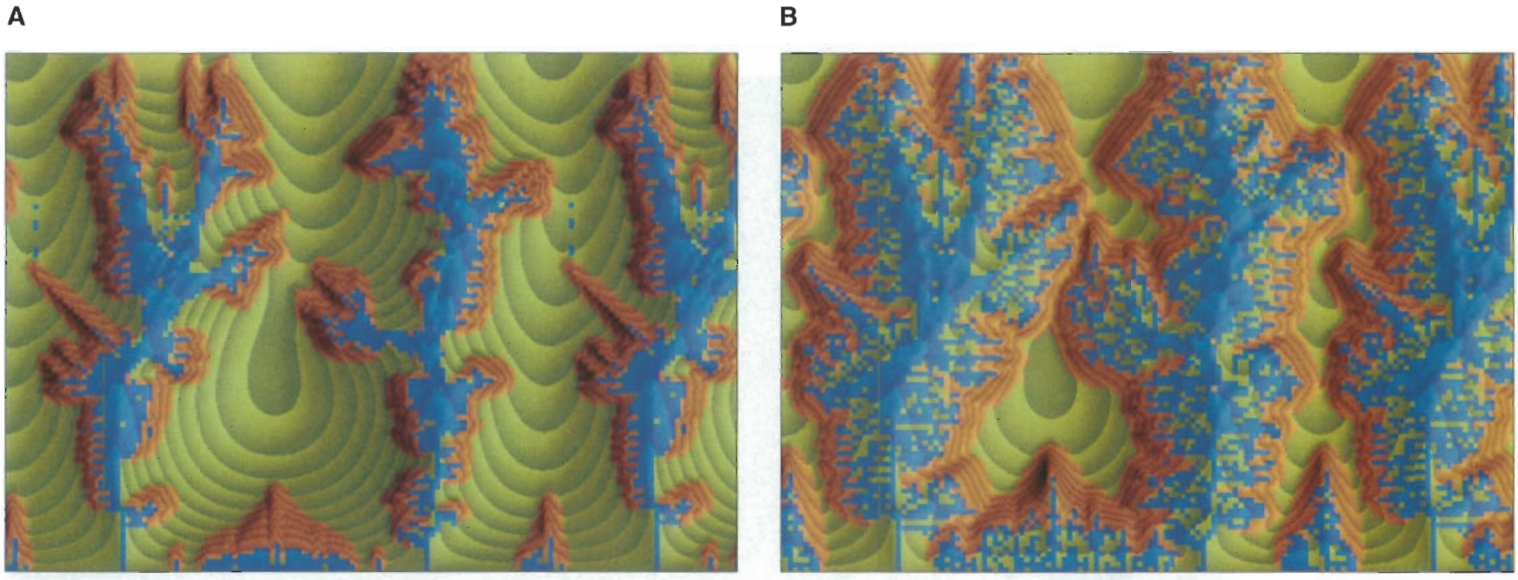

Figure 11.4 Simulation of gullying and valley sedimentation when the regolith or bedrock is strongly erodible (A) at time $T = 0.14$ after the initial threshold lowering (the duration of the threshold lowering was $T_d = 0.01$); (B) at time $T = 0.39$. Colour-coding is green for areas of normal erosion, brown for areas of accelerated erosion, and blue for areas of alluviation.

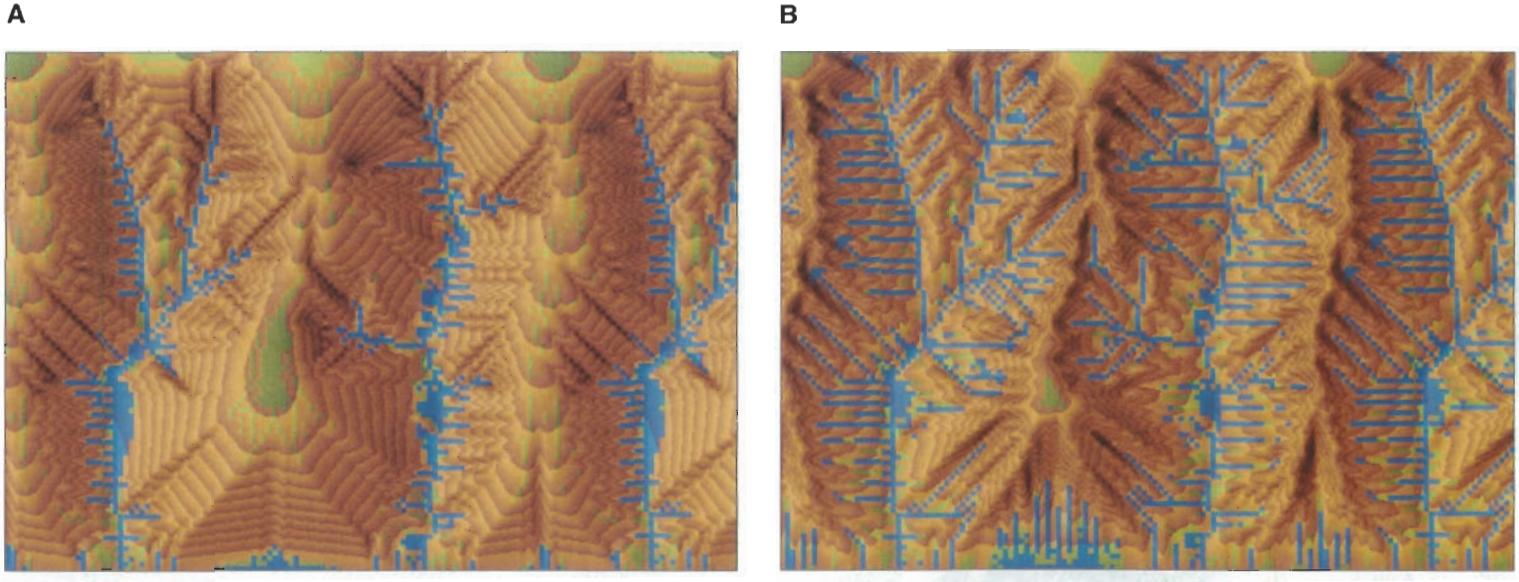

Figure 11.5 Simulation of gullying and badland slope development following a very large reduction in critical shear stress for fluvial erosion. Duration of threshold lowering $T_d = 0.05$. (A) at $T = 0.19$; (B) at $T = 0.51$.

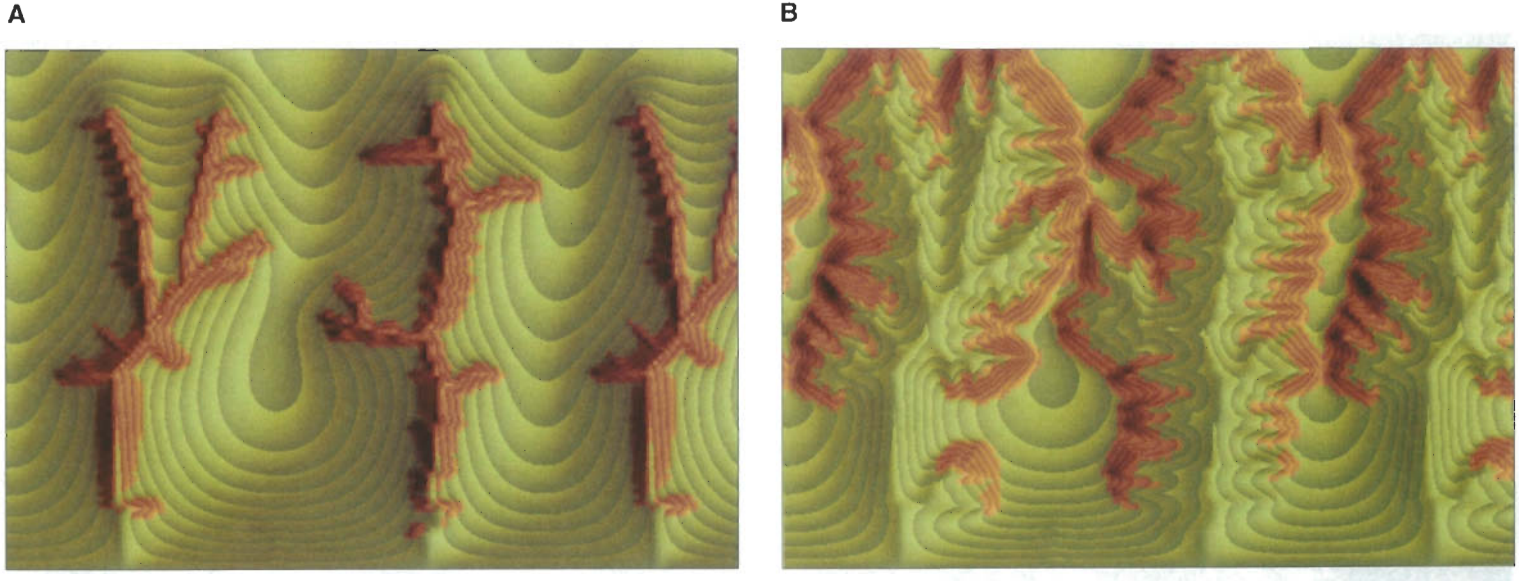

Figure 11.6 Simulation of gullying when the regolith is not highly erodible. Note that the lower slopes and channels revert to the normal erosional state after passing of the zone of accelerated erosion. Duration of threshold lowering, $T_d = 0.05$. (A) at $T = 0.65$; (B) at $T = 6.0$.

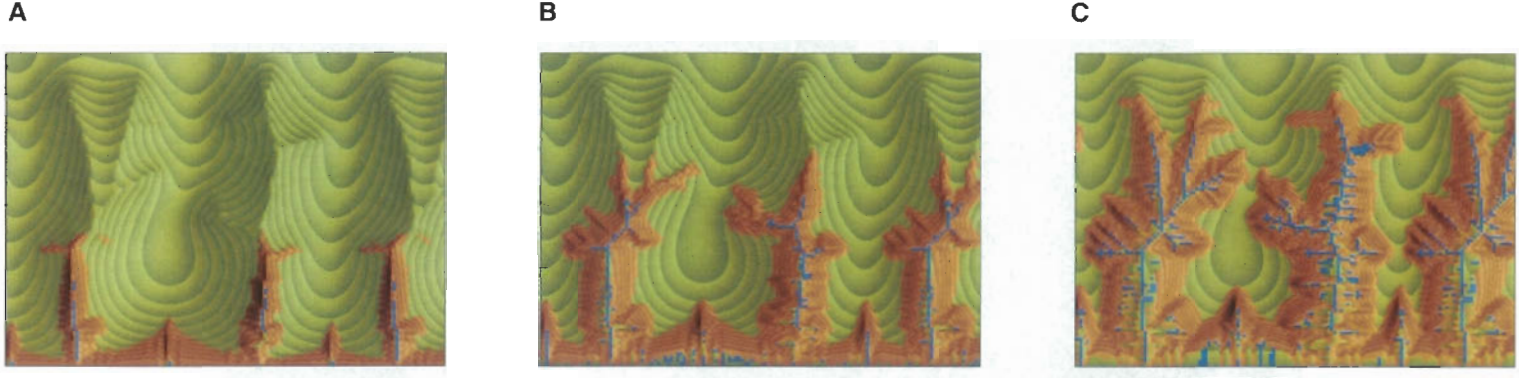

Figure 11.7 Simulation of headcut advance following a rapid lowering of the master stream level at the lower boundary. Starting from the steady state landscape (Figure 11.2), the lower boundary was lowered at an erosion rate of $E = 160$ for a duration $\Delta T = 0.25$ (A) at time $T = 0.28$; (B) at time $T = 0.49$; (C) at time $T = 0.74$.

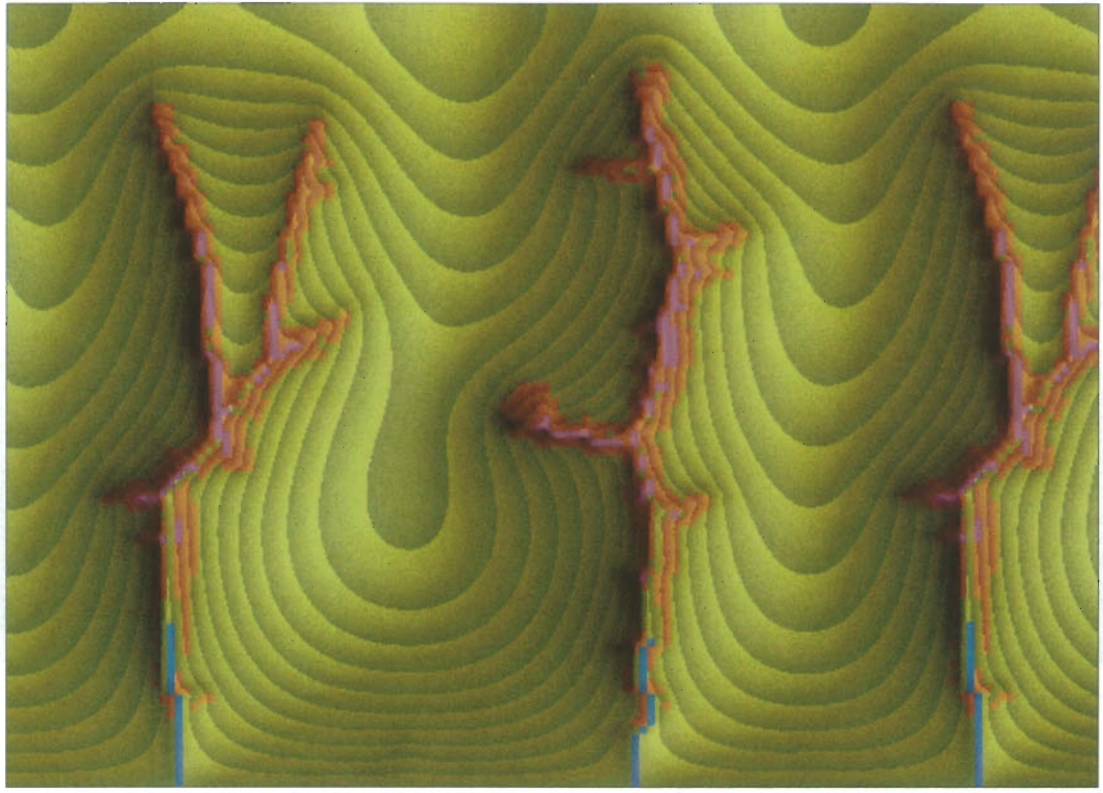

Figure 11.8 Simulation of gullying into shallow regolith (thickness = 25) so that bedrock (purple) becomes exposed at the bottom of the gullies and the rate of advance of the gully headwall is slowed. Duration of threshold lowering, $T_d = 0.03$. Results are shown at time $T = 1.11$.